

# Part2Word: Learning Joint Embedding of Point Clouds and Text by Matching Parts to Words

Chuan Tang  
School of Artificial Intelligence, Jilin  
University  
Changchun, China  
tangchuan1998@gmail.com

Xi Yang  
School of Artificial Intelligence, Jilin  
University  
Changchun, China  
earthyangxi@gmail.com

Bojian Wu  
Alibaba Group  
Hangzhou, China  
ustcbjwu@gmail.com

Zhizhong Han  
Department of Computer Science,  
Wayne State University  
Detroit, USA  
h312h@wayne.edu

Yi Chang  
School of Artificial Intelligence, Jilin  
University  
Changchun, China  
yichang@jlu.edu.cn

## ABSTRACT

It is important to learn joint embedding for 3D shapes and text in different shape understanding tasks, such as shape-text matching, retrieval, and shape captioning. Current multi-view based methods learn a mapping from multiple rendered views to text. However, these methods can not analyze 3D shapes well due to the self-occlusion and limitation of learning manifolds. To resolve this issue, we propose a method to learn joint embedding of point clouds and text by matching parts from shapes to words from sentences in a common space. Specifically, we first learn segmentation prior to segment point clouds into parts. Then, we map parts and words into an optimized space, where the parts and words can be matched with each other. In the optimized space, we represent a part by aggregating features of all points within the part, while representing each word with its context information, where we train our network to minimize the triplet ranking loss. Moreover, we also introduce cross-modal attention to capture the relationship of part-word in this matching procedure, which enhances joint embedding learning. Our experimental results outperform the state-of-the-art in multi-modal retrieval under the widely used benchmark.

## CCS CONCEPTS

• **Computing methodologies** → **Visual content-based indexing and retrieval; Learning latent representations.**

## KEYWORDS

joint embedding, point cloud, text, matching

## 1 INTRODUCTION

Large 3D models with rich details have been available for 3D deep learning research and applications [3, 31]. Beyond 3D shapes themselves, text descriptions provide additional information, and make people convenient to retrieve and use these massive 3D models. However, it is hard to jointly understand 3D shapes and text at the same time due to the different modalities, which makes it challenging to represent both of them in a common semantic space.

The state-of-the-art methods aim to map different 3D representations into a learned joint embedding space with text, such as voxel grids [4] and multiple views [12, 13]. However, both voxel grids

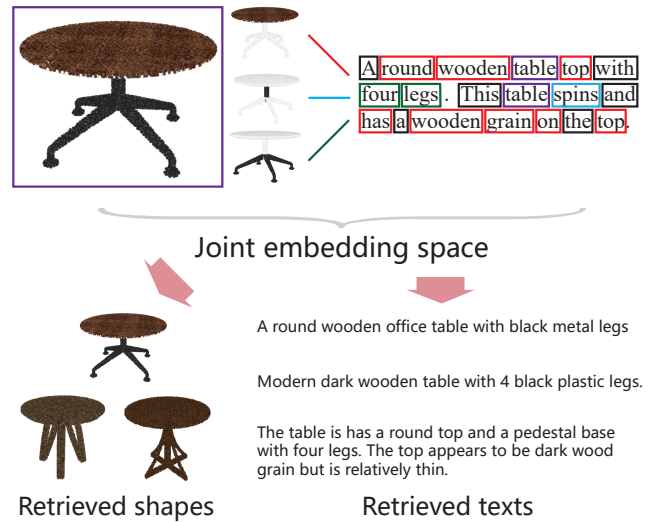


**Figure 1: We propose a method to learn the joint embedding of point clouds and text by matching parts to words. Using the learned joint embedding, we can either retrieve shapes using sentences or retrieve sentences using shapes.**

and multiple views make these methods struggle to improve the ability of joint understanding of shapes and text, due to the lack of shape information caused by low-resolution of voxel grids and self-occlusion in multiple views.

Learning a joint embedding of 3D shapes and text is a promising solution to overcome this challenge. However, due to the different representation of 3D shapes, such as existing methods that leverage voxel grids [4] and multiple views [12, 13], it is hard to learn an expressive embedding of 3D shape, because of the lack of 3D information caused by low-resolution of voxels and self-occlusion in multiple views, which will directly lead to the unsatisfactory joint understanding of shapes and text.

To resolve this issue, we propose a point-based multi-modal alignment network to learn the joint embedding of point clouds and text. To leverage more local shape information, our network

is trained to match parts on point clouds to words in sentences. Specifically, we first learn segmentation prior to segment point clouds into parts. Then, we map parts and words into an optimized space, where the parts and words can be matched with each other. In the optimized space, we represent a part by aggregating features of all points within the part, while representing each word with its context information, where we train our network to minimize the triplet ranking loss. Moreover, we also introduce cross-modal attention to capture the relationship of part-word in this matching procedure, which enhances joint embedding learning. Experimental results show that our method can significantly improve the shapes and text understanding ability. Our contributions are listed below,

- We propose a novel network framework for the matching of text description of 3D shapes based on points with the features of semantic segmentation.
- Comparing with the existing methods, our proposed network achieves SOTA results for matching 3D shapes with text description on various evaluation metrics.
- We demonstrated retrieval and visualization results to further illustrate the effectiveness of our proposed network.

## 2 RELATED WORK

We review work in related areas such as multi-model representation learning of shapes and text, deep learning of 3D point clouds and text related matching tasks.

### 2.1 Joint embedding of 3D shapes and text

In a recent pioneering work, Chen et al. [4] introduce a novel 3D-Text cross-modal dataset by annotating each 3D shape from ShapeNet [3] with neural language description. In order to understand the inherent connections between text and 3D shapes, they employ CNN+RNN and 3D-CNN to extract features from freeform text and 3D voxelized shapes respectively. It uses full multi-modal loss to learn the joint embedding and calculate similarity between both modal features. However, due to the complexity of computational 3D convolutions, it is hard to generalize this model to high-resolution. To resolve this issue, Han et al. [13] propose  $Y^2Seq2Seq$ , which is a view-based method, to learn cross-modal representations by joint reconstruction and prediction of view and word sequences. Although this method can extract texture information from multiple rendered views by CNN and acquire global shape representation by RNN, it ignores local information aggregation such as part-level features of 3D shapes, which proves to be useful for 3D-Text task. To take a step further, Han et al. [12] propose to detect shape parts on 2D rendered images, but it is still struggling to fully understand 3D shapes due to the inaccurate boundaries and self-occlusion. Differently, our method directly learns from point clouds sampled from shapes, which could better preserve the intrinsic 3D properties, and therefore obtains more discriminative features.

### 2.2 Point-based 3D deep learning

Point clouds have been an important representations of 3D shapes due to its simplicity and compactness. PointNet [32] and PointNet++ [33] are the pioneer works to understand this kind of irregular data. After that, lots of studies [27, 39] are proposed to

improve the interpretability of network for point clouds in different tasks, such as segmentation [28, 29, 37], classification [28, 29, 37], reconstruction [9, 11, 14, 18], completion [15, 16, 38]. Besides, the learned deep features of a single point or the whole shape could also be applied to 3D shape based cross-modal applications, for example, shape-to-text matching in our case. In detail, we learn a segmentation prior to segment point clouds into multiple parts, the point-level features of parts will be further aggregated and then matched with words from text.

### 2.3 Image-text matching

Image-text matching task allows image or text to mutually find the most relevant instance from the multi-modal database. Most existing methods can be roughly categorized into two types: global matching methods and regional matching methods.

**Global matching methods**[30] aim to extract the global representation from both images and texts, and then calculate the similarity score. Kiros et al. [24] force image and text to be mapped to the same embedding space by optimizing pairwise ranking loss. Faghri et al. [8] try to improve the performance by exploiting the hard negative mining strategy during training. Chen et al. [5] train models by a combination of online triplet loss and offline quintuplet loss. Zhang et al. [42] propose a CPM loss and a CMPC loss to learn a discriminative image-text embedding. The key of these works is to use different loss functions to project image and text into the same embedding space. Besides, Wang et al. [35] and Gu et al. [10] use generative model to learn textual-visual feature embedding in a common representational space.

**Regional Image-Text Matching** first extract image region representation from existing detectors and then take latent visual-semantic correspondence at the level of image regions and words into consideration. Karpathy et al. [21, 22] propose visual semantic matching through inferring their inter-modal alignment, these methods first detect object regions and then acquire the region-word correspondence, finally aggregate the similarity of all possible pairs of image regions and words in sentence to infer the global image-text similarity. Inspired by [1], SCAN [25] takes a step towards attending to important image regions and words with each other as context for inferring the image-text similarity. Recently, some works [6, 17, 20, 26, 36, 40] attempt to improve SCAN and try to achieve better performance.

## 3 OUR METHOD

Inspired by the framework of SCAN [25], we introduce a cross-attention mechanism to learn the joint embedding of 3D shapes and text by matching parts from shapes to words from sentences. Note that, compared with ShapeCaptioner [12] which learns the regional representation from multi-view images, our method directly utilizes point clouds as the intermediate representation of 3D shapes, and learns deep embedded features of 3D parts obtained by point cloud segmentation, which is a key difference from previous methods.

**Overview.** We design a network to complete the 3D shape-text matching task, as shown in Figure 2. The proposed network includes three modules: shape encoder, text encoder, and matching module. To encode a 3D shape  $S$ , we use a pre-trained segmentation network to obtain the intermediate representation of each sampling

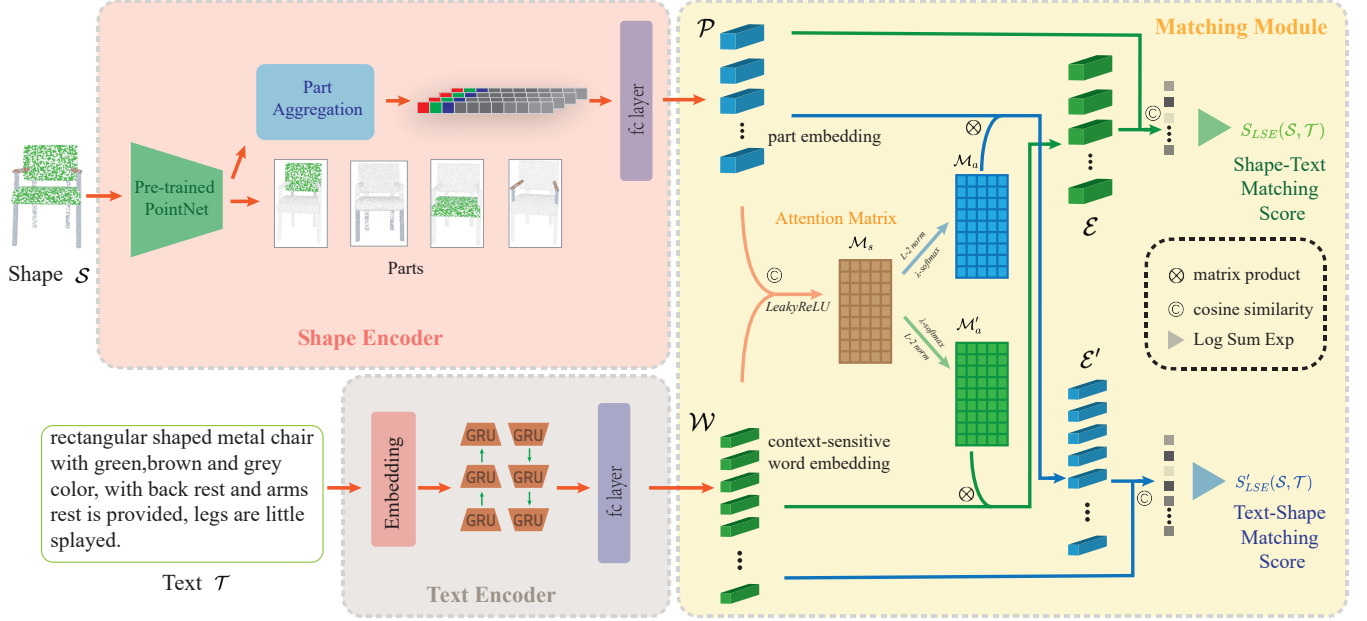


**Figure 2: Overview of our proposed network. The proposed network includes three modules: shape encoder, text encoder, and matching module. The shape encoder learns the part embedding from input 3D shapes, and the text encoder learns the word embedding from the corresponding text description. Then, we utilize the alignment-based cross attention module to predict a pair of symmetrical formulations, shape-text and text-shape, to achieve the matching of parts with words.**

point on the input surface model. Then, we aggregate these representations to extract the part embedding  $\mathcal{P} \in \{p_1, p_2, \dots, p_k\}$  of the input shape  $\mathcal{S}$ . For the text encoder, we use the Bi-directional Gate Recurrent Unit (GRU) to learn context sensitive embedding  $\mathcal{W} \in \{w_1, w_2, \dots, w_m\}$  of each word in the sentence  $\mathcal{T}$ . To achieve the matching between  $\mathcal{P}$  and  $\mathcal{W}$ , we employ an alignment-based matching module, which uses cross attention to align parts with words and acquire similarity score. The module contains a pair of symmetrical formulations which are denoted as Shape-Text and Text-Shape.

### 3.1 Shape Encoder

Our shape encoder extracts the embedding of parts on each input shape by aggregating the features of corresponding points on the segmented parts, as shown in Figure 3. We firstly feed  $\mathcal{S}$  to a pre-trained point-based segmentation network (using PointNet [32] in our case) to extract the features of each point. Besides the coordinates, we also incorporate the color information of each point in the shape encoder. Then, we concatenate the outputs  $f^1, f^2, f^3$  of the last three layers of PointNet to form the embedding of parts, which includes the information from the different semantic hierarchies. Moreover, we also concatenate the color representation  $color$  of the input shape to leverage the color information. We ignore the part which contains less than 25 points, and limit the number of segmented parts is not larger than  $\kappa$  for each input shape. Then, we feed the aggregated features and part segmentation information into a Group Average Pooling layer to extract the part embedding  $\mathcal{P}$  of each part.

### 3.2 Text Encoder

For the text encoder, we use Bi-directional GRU to extract the context-sensitive word embedding  $\mathcal{W}$ . Each text description  $\mathcal{T}$  is first represented by the embedding of each single word in the sentence through a word embedding layer, where the embedding of each single word is also simultaneously learned with other parameters in the network. Then, we encode the context of each single word in the bi-directional GRU. For the forward GRU, the hidden state at position  $i$  can be calculated from the word embedding at position  $i$  and the hidden state at position  $i - 1$ . Similarly, for the reverse GRU, the hidden state at position  $i$  is calculated from the word embedding at position  $i$  and the hidden state at position  $i + 1$ . Finally, the context-sensitive word embedding is obtained by the averages of the hidden states in the two directions.

### 3.3 Matching

Shape-Text matching module matches the input 3D shape  $\mathcal{S}$  and text  $\mathcal{T}$  by the part embedding  $\mathcal{P}$  and context-sensitive word embedding  $\mathcal{W}$  respectively extracted by our shape encoder and text encoder. Note that the part embedding first needs to go through a single fully connected layer to ensure that it has the same dimensions as the word embedding. Then, we introduce cross attention to compute two symmetrical formulations: Shape-Text matching score, and Text-Shape matching score.

For the Shape-Text matching, we firstly use cross attention to build the relationship between parts and words. We compute cosine similarity between  $\mathcal{P}$  and  $\mathcal{W}$  to obtain the attention matrix  $\mathcal{M}^s$ , and use LeakyReLU to weaken the impact of negative values, as shown

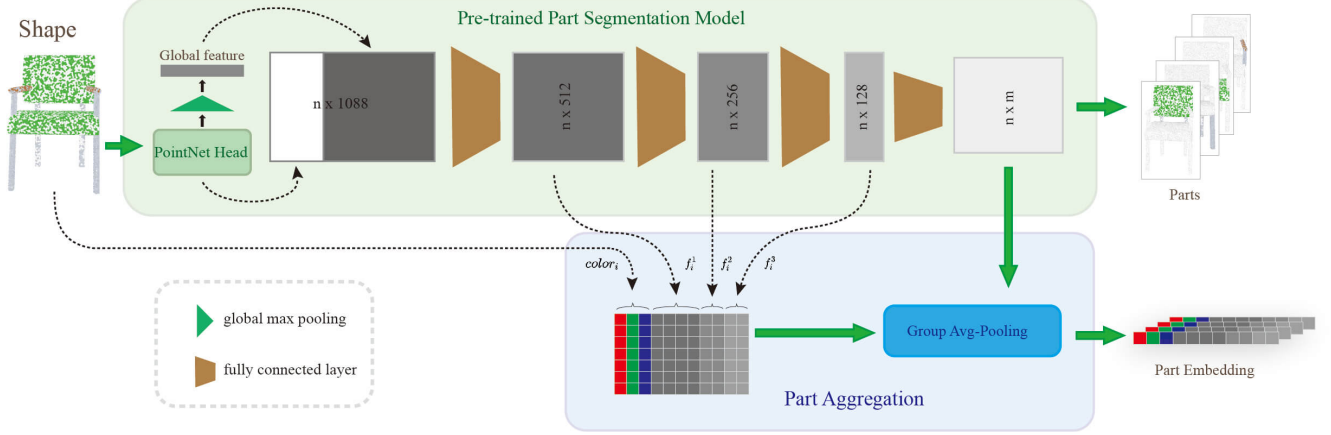


**Figure 3: Shape Encoder.** We aggregate the outputs of the last three layers of PointNet and color information to represent the embedding of parts.

in Eq. (1). Then, the attention matrix  $\mathcal{M}^s$  is normalized by part-wise L-2 normalization in Eq. (2) and word-wise  $\lambda$ -softmax function in Eq. (3), where  $\lambda$  is the inversed temperature of the softmax function [7]. After that, we multiple the normalized attention matrix  $\mathcal{M}^s$  and context-sensitive word embedding  $\mathcal{W}$  to obtain the attention sentence embedding  $\mathcal{E}$  corresponding to each shape part in Eq. (4).

$$\mathcal{M}_{ij}^s = \text{LeakyReLU} \left( \frac{p_i^T w_j}{\|p_i\| \|w_j\|}, 0.1 \right), i \in [1, k], j \in [1, m] \quad (1)$$

$$\mathcal{M}_{i,j}^a = \frac{\mathcal{M}_{i,j}^s}{\sqrt{\sum_{i=1}^k (\mathcal{M}_{i,j}^s)^2}}, \quad (2)$$

$$\mathcal{M}_{ij}^a = \frac{\exp(\lambda_1 \mathcal{M}_{i,j}^a)}{\sum_{j=1}^m \exp(\lambda_1 \mathcal{M}_{i,j}^a)} \quad (3)$$

$$\mathcal{E}_i = \sum_{j=1}^m \mathcal{M}_{i,j}^a \mathcal{W}_j \quad (4)$$

Finally, we calculate the cosine similarity between  $\mathcal{P}$  and  $\mathcal{E}$  to represent the relationship between parts and sentences in Eq. (5). And the final Shape-Text similarity score is obtained through the LogSumExp pooling, as shown in Eq. 6.

$$R(p_i, e_i) = \frac{p_i^T e_i}{\|p_i\| \|e_i\|}, i \in [1, k] \quad (5)$$

$$S_{LSE}(S, T) = \log \left( \sum_{i=1}^k \exp(\lambda_2 R(p_i, e_i)) \right)^{(1/\lambda_2)} \quad (6)$$

Similarly, the Shape-Text matching score  $S_{LSE}(T, S)$  can be calculated by reversing the embedding of parts and words.

### 3.4 Objective Function

We use paired ranking loss in our objective function, as shown in Eq. (8). To facilitate the network to better converge and avoid getting into collapsed model, we employ the semi-hard negative sampling mining strategy [34]. Specifically, for a positive sampling pair  $(S, T)$ , we select the hardest negative sampling pair  $(\hat{S}_{semi}, \hat{T}_{semi})$  which has a smaller similarity score than  $(S, T)$ , and calculate the triplet loss for the input shape and text respectively. Similarly, the triplet loss between the sampling pair  $(T, S)$  can also be calculated in the same way. The triplet loss for both pairs of  $(S, T)$  and  $(T, S)$  is defined below, here  $\alpha$  is a margin that is enforced between positive and negative pairs.

$$\begin{aligned} L(S, T) &= [\alpha - S_{LSE}(S, T) + S_{LSE}(S, \hat{T}_{semi})]_+ + \\ &\quad [\alpha - S_{LSE}(S, T) + S_{LSE}(\hat{S}_{semi}, T)]_+ \\ L(T, S) &= [\alpha - S_{LSE}(T, S) + S_{LSE}(T, \hat{S}_{semi})]_+ + \\ &\quad [\alpha - S_{LSE}(T, S) + S_{LSE}(\hat{T}_{semi}, S)]_+ \end{aligned} \quad (7)$$

In summary, we train our network by minimizing the following loss function, where  $\beta$  is a balance weight and we set  $\beta = 1$  in all our experiments.

$$L = L(S, T) + \beta L(T, S) \quad (8)$$

## 4 EXPERIMENTS

We conducted comparison experiments to evaluate the performance of our proposed network on widely used benchmarks. We first introduce the benchmark [3, 4, 31], evaluation metric as well as the parameter setting of our proposed network, then we report the comparison results with the SOTA methods. We also show the results of ablation studies to explain the design of our proposed network. Finally, we explore the relationship between parts and words by visualizing the attention learned in our network.

**Dataset and metrics.** We evaluate our proposed network on 3D-Text cross-modal dataset [4]. However, this dataset does not



Figure 4: Results of our proposed network on the S2T and T2S retrieval tasks. In each case, the corresponding ground-truths are marked in red.

include 3D point clouds and the segmentation prior. To resolve this challenge, we employed two additional datasets, ShapeNet [3] and PartNet [31], which share the same 3D models. ShapeNet [3] contains different 3D representations, including point clouds with color, but no segmentation annotation. PartNet [31] contains fine-grained, instance-level, and hierarchical 3D part information which is manually annotated. However, the PartNet does not contain color information of 3D point clouds. To leverage the color information of 3D point clouds and the part segmentation annotation at the same time, we perform point cloud registration [2] on both point cloud models make an alignment, then we annotate segmentation labels on the point clouds of ShapeNet by the nearest annotated

neighbor points on PartNet. Finally, We use 11498 3D shapes for training and 1434 3D shapes for testing contains chairs and tables. Each 3D shape has an average of 5 text descriptions.

For the evaluation metrics, we employ recall rate (RR@k) and NDCG [19] to conduct quantitative evaluation.

**Parameter Setting.** We train the two networks (segmentation network and matching network) separately on the same dataset. For the point cloud segmentation network, 2500 points are randomly sampled from point clouds with 10000 points to represent a shape. For training, Adadelta [41] is used as the optimizer, the batch size is set to 32, the learning rate is set to 0.01, and the training epoch is 300. In the matching network, with comparison experiments, we set

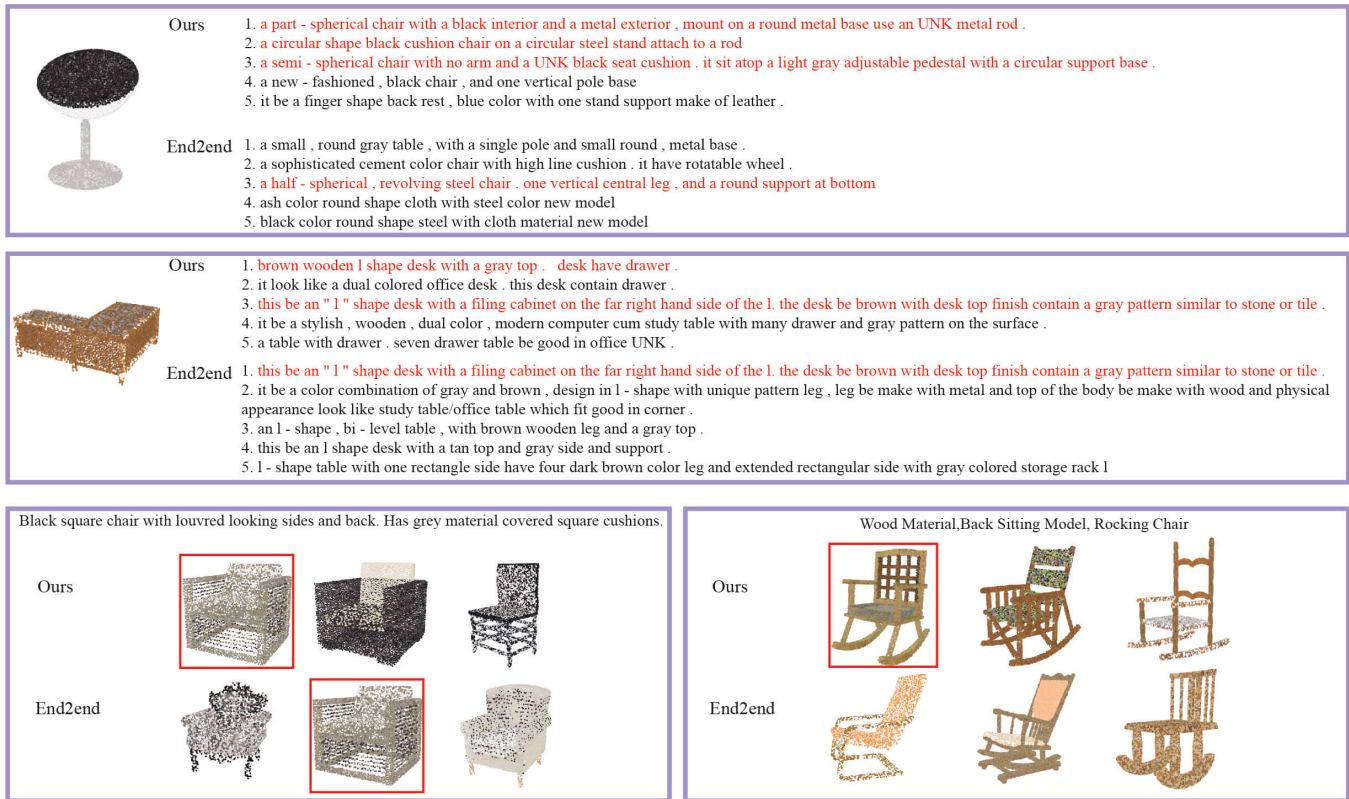


Figure 5: Comparison with an end2end network that only extracted global shape features, on the S2T and T2S retrieval tasks.

the max number  $\kappa$  of parts on each shape as 5, and the dimension of part embedding we feed into the matching module as 1024. we set the dimension of word embedding to 300 and the hidden state dimension to 1024, which is consistent with [12, 13]. We also use the vocabulary of 3587 unique words and a single layer bi-direction GRU as the text encoder. For the loss function, we adopt semi-hard negative mining strategy, and the margin  $\alpha$  of triplet ranking loss is set to 0.2. For training, we use the Adam [23] optimizer and set the learning rate to 0.001.

#### 4.1 Comparison with SOTA methods

Table 1 presents the quantitative results on ShapeNet where our method outperforms the existing approaches [4, 13] in all measures. To compare the local part information with the global shape information, we designed an end-to-end model, which simply uses PointNet as the point cloud global feature encoder, Bi-GRU as the text encoder, and also uses semi-hard negative mining triplet ranking loss to train the network. We also take different formulation of cross attention into consideration, where S-T represents Shape-Text formulation, T-S represents Text-Shape formulation, and T-S + S-T represents the average of two predicted similarity scores. Our results experimentally demonstrate that our method achieves significantly better performance than the end-to-end method using global information. Compared with the state-of-the-art methods, our best RR@1 is almost one time better than the results of Y2Seq2Seq in both shape-to-text retrieval and text-to-shape retrieval task.

Table 1: Retrieval results on Text2Shape dataset (ShapeNet subset) compared with the state-of-the-art methods.

	Method	Recall@1	Recall@5	NDCG@5
S2T	Text2Shape	0.83	3.37	0.73
	Y2Seq2Seq	6.77	19.30	5.30
	end2end	9.55	28.45	8.01
	T-S + S-T (Ours)	11.44	32.01	8.91
	S-T (Ours)	11.65	32.57	9.45
	T-S (Ours)	<b>13.18</b>	<b>34.52</b>	<b>9.94</b>
T2S	Text2Shape	0.40	2.37	1.35
	Y2Seq2Seq	2.93	9.23	6.05
	end2end	7.13	22.63	14.94
	T-S + S-T (Ours)	6.65	21.28	14.12
	S-T (Ours)	7.02	21.46	14.34
	T-S (Ours)	<b>7.94</b>	<b>23.89</b>	<b>16.03</b>

The examples of T2S and S2T retrieval results are shown in Figure 4. For the S2T retrieval task, our proposed model is employed to retrieve the top-5 matched sentences. Symmetrically, for the T2S retrieval task, our proposed network is employed to find the top-5 matched 3D shapes. In this figure, we mark the ground-truth text descriptions of the corresponding shapes in red.

**Table 2: Performance of selecting different  $m$  for segmentation granularity.**

	Metrics	17	72	90	44
S2T	Recall@1	8.23	11.79	12.34	<b>13.18</b>
	Recall@5	26.99	29.92	33.82	<b>34.52</b>
	NDCG@5	6.88	8.78	9.51	<b>9.94</b>
T2S	Recall@1	5.77	6.79	7.44	<b>7.94</b>
	Recall@5	18.65	22.1	22.14	<b>23.89</b>
	NDCG@5	12.19	14.6	14.84	<b>16.03</b>

**Table 3: Comparison of different negative sample learning strategies based on triplet ranking loss.**

	Method	Recall@1	Recall@5	NDCG@5
S2T	Triplet Loss	8.58	28.24	7.44
	HNM	4.46	13.32	3.55
	Semi-hard	<b>13.18</b>	<b>34.52</b>	<b>9.94</b>
T2S	Triplet Loss	6.75	20.83	13.82
	HNM	1.97	7.83	4.89
	Semi-hard	<b>7.94</b>	<b>23.89</b>	<b>16.03</b>

## 4.2 Ablation Study

We first explore the impact of part embedding extracted under different segmentation granularities on the matching model. The PartNet dataset contains hierarchical segmentation annotation of 24 object categories. Meanwhile, for the text-3D shape matching task, we only need the object and segmentation labels of the two categories of chair and table. Therefore, we can obtain semantic segmentation annotations of 17, 72, and 90 categories from coarse level to fine-grained level part semantic segmentation, respectively. In addition, we also created a 44-category semantic segmentation annotation by merging too detailed semantic parts. We employ PointNet to learn the part segmentation model from these four segmentation granularities  $m$ ,  $m \in \{17, 44, 72, 90\}$ . As shown in Table 2, we can find that the part embedding obtained from the 44-category segmentation model achieves the best results on the matching task. Through the results of the above experiments, we believe that the predicted segmentation results will become inaccurate, and many segmentation parts are redundant for matching when we employ fine-grained level part segmentation annotation. When using coarse level part segmentation, the learned segmentation network has more accurate segmentation results, but the obtained part embedding will ignore the details corresponding to the shape caption. Therefore, we need to find a balance between the accuracy and the semantic abundance of the segmentation model. In the following, we set the  $m$  to 44.

Next, we explore the impact of different negative sample learning strategies based on triplet ranking loss on retrieval. As shown in Table 3, we compared three strategies: basic strategy, hardest negative mining, and semi-hard negative mining. The basic strategy (Triplet Loss) averages over all the triplet ranking loss of each negative pair in a mini-batch. The hardest negative mining strategy (HNM)

**Table 4: Ablation study on part aggregation operation.**

	Method	Recall@1	Recall@5	NDCG@5
S2T	w/o RGB	11.58	30.89	8.81
	Single layer	11.65	32.71	9.03
	Max	11.92	<b>35.5</b>	<b>9.96</b>
	Ours	<b>13.18</b>	34.52	9.94
T2S	w/o RGB	7.41	21.4	14.49
	Single layer	7.14	21.38	14.37
	Max	7.61	<b>24.07</b>	15.97
	Ours	<b>7.94</b>	23.89	<b>16.03</b>

only focuses on the triplet ranking loss of the hardest negative pair, and the semi-hard negative mining (Semi-hard) selects the negative sample pair which does not exceed the score of the positive sample pair in a mini-batch. Our experimental results show that the semi-hard negative mining strategy achieves better performance in all metrics.

Table 4 shows the effectiveness of our proposed part aggregation operation. We experimentally prove the necessity of explicitly adding color information by comparing the matching results with part color concatenated to part embedding. We improve NDCG@5 about 1.13 and 1.54 separately in S2T and T2S tasks after explicitly using color information. The results indicate that we should to explicitly concatenate the color information of each part to part embedding, although the point color is involved as a part of the input of the segmentation network. Besides, to compare the performance of our aggregation with the embeddings of different hierarchies, we attempt to replace the concatenated embedding with the feature of the last fully connected layer. For a fair comparison, color information is also explicitly added to the part embedding. The result shows that the NDCG@5 with our aggregation improves 0.91 and 1.66 in the S2T task and T2S task, respectively. We also compare the max pooling with the mean pooling, the results show that mean pooling can slightly improve Recall@1 in S2T and T2S task. These experiments demonstrate the effectiveness of our proposed aggregation.

## 4.3 Visualization

To interpret our proposed network, we visualize the intermediate results of cross attention matching module, as shown in Figure 6. Given pair of shape and text, we use our proposed Part2Word matching model to acquire the attention weight between parts and words. The correlation between each word of the input text and each part of the input shape is visualized by controlling their transparency using the corresponding attention weights. A visualization example is shown in Figure 6. The chair first is divided into 5 parts by trained part segmentation network, and then we use the Part2Word model to calculate the attention weights. By analyzing the visualization results, we can find the black seat part matches word "black" and "seat" in the sentence well, and the part of yellow and black rest also attend the words "yellow", "black" and "rest". Besides, the attention weight between the part of blue legs and the word "blue" obtained the highest score.

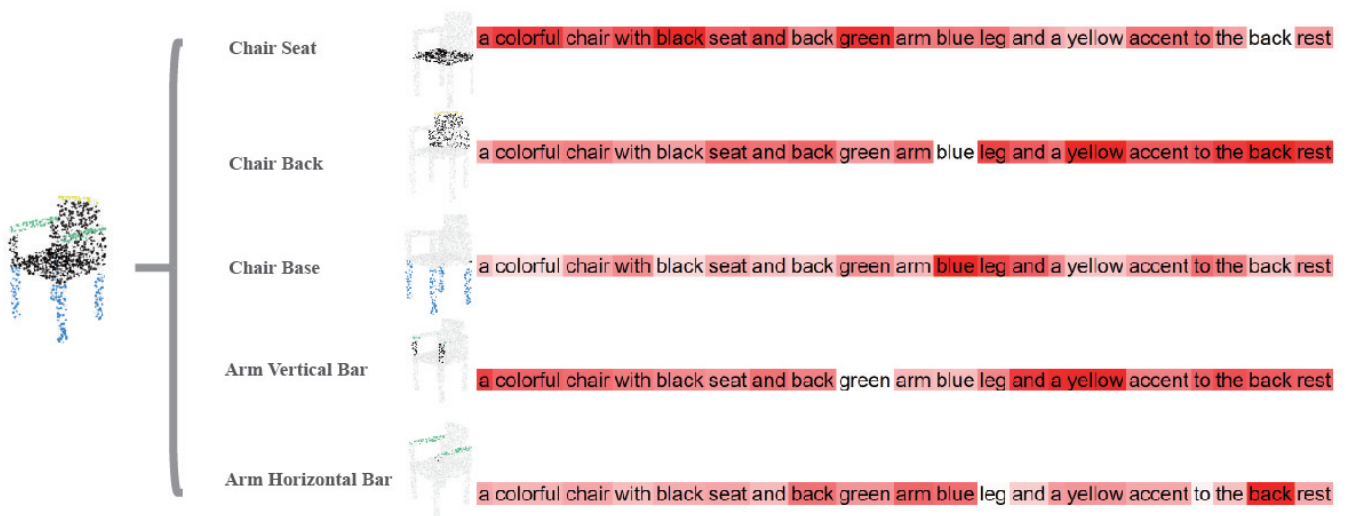


Figure 6: Attention visualization. We visualize the attention weight to show the relationship between a part and each word in the sentence. The color of red indicates large attention weights.

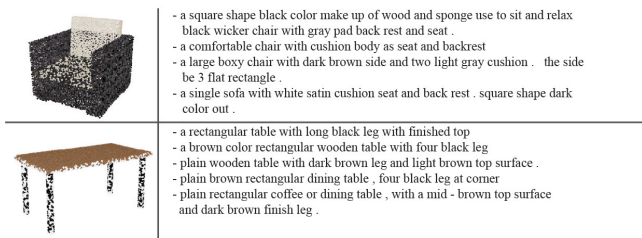


Figure 7: The groundtruth of point clouds from ShapeNet show disordered color.

## 5 LIMITATION

Although our experimental results demonstrated the proposed network is significantly better than the existing networks, this is the baseline of the point-based matching network since we use PointNet segmentation network to extract the part embedding. The performance can be improved greatly by using other advanced point-based networks. For the ShapeNet dataset, we found they have color problems on a large number of point cloud data, as shown in Figure 7. The color of points is not correct, it may be caused by data processing mistakes. Therefore, noise information is involved in our network and affected our final results. Finally, comparing with multi-views based approaches, the point-based method should carefully distinguish the difference between the original color of points and rendered color of them. And the sparse sampling points may hard to exactly represent the surface color because of the highlights and shadows, according to different rendering environments.

## 6 CONCLUSION

We introduce a method to learn joint embedding of 3D point clouds and text. Our method successively increases the joint understanding of 3D point clouds and text by learning to match 3D parts to words

in an optimized space. We obtain the 3D parts by leveraging a 3D segmentation prior, which effectively resolves the self-occlusion issue of parts that suffers current multi-view based methods. We also demonstrate that matching 3D parts to words is a good way to merge different modalities including 3D shapes and text in a common space, where the proposed cross-modal attention is also justified to effectively capture the relationship of part-word in this matching procedure. Experimental results show that our method outperforms other state-of-the-art methods.

## REFERENCES

- [1] Peter Anderson, Xiaodong He, Chris Buehler, Damien Teney, Mark Johnson, Stephen Gould, and Lei Zhang. 2018. Bottom-Up and Top-Down Attention for Image Captioning and Visual Question Answering. In *Proc. IEEE Conf. on Computer Vision & Pattern Recognition*. 6077–6086.
- [2] Paul J. Besl and Neil D. McKay. 1992. A Method for Registration of 3-D Shapes. *IEEE Trans. Pattern Analysis & Machine Intelligence* 14, 2 (1992), 239–256.
- [3] Angel X. Chang, Thomas Funkhouser, Leonidas Guibas, Pat Hanrahan, Qixing Huang, Zimo Li, Silvio Savarese, Manolis Savva, Shuran Song, Hao Su, Jianxiong Xiao, Li Yi, and Fisher Yu. 2015. *ShapeNet: An Information-Rich 3D Model Repository*. Technical Report arXiv:1512.03012 [cs.GR]. Stanford University – Princeton University – Toyota Technological Institute at Chicago.
- [4] Kevin Chen, Christopher B Choy, Manolis Savva, Angel X Chang, Thomas Funkhouser, and Silvio Savarese. 2018. Text2shape: Generating shapes from natural language by learning joint embeddings. In *Proc. Asian Conf. on Computer Vision*. 100–116.
- [5] Tianlang Chen, Jiajun Deng, and Jiebo Luo. 2020. Adaptive Offline Quintuplet Loss for Image-Text Matching. In *Proc. Euro. Conf. on Computer Vision*, Vol. 12358. 549–565.
- [6] Tianlang Chen and Jiebo Luo. 2020. Expressing Objects Just Like Words: Recurrent Visual Embedding for Image-Text Matching. In *Proc. AAAI Conference on Artificial Intelligence*. 10583–10590.
- [7] Jan Chorowski, Dzmitry Bahdanau, Dmitriy Serdyuk, Kyunghyun Cho, and Yoshua Bengio. 2015. Attention-Based Models for Speech Recognition. In *Advances in Neural Information Processing Systems*, Corinna Cortes, Neil D. Lawrence, Daniel D. Lee, Masashi Sugiyama, and Roman Garnett (Eds.), 577–585.
- [8] Fartash Faghri, David J. Fleet, Jamie Ryan Kiros, and Sanja Fidler. 2018. VSE++: Improving Visual-Semantic Embeddings with Hard Negatives. In *Proc. British Machine Vision Conference*.
- [9] Thibault Groueix, Matthew Fisher, Vladimir G. Kim, Bryan C. Russell, and Mathieu Aubry. 2018. A Papier-Mâché Approach to Learning 3D Surface Generation. In *Proc. IEEE Conf. on Computer Vision & Pattern Recognition*.



- [10] Jiuxiang Gu, Jianfei Cai, Shafiq R. Joty, Li Niu, and Gang Wang. 2018. Look, Imagine and Match: Improving Textual-Visual Cross-Modal Retrieval With Generative Models. In *Proc. IEEE Conf. on Computer Vision & Pattern Recognition*. 7181–7189.
- [11] Zhizhong Han, Chao Chen, Yu-Shen Liu, and Matthias Zwicker. 2020. DRWR: A Differentiable Renderer without Rendering for Unsupervised 3D Structure Learning from Silhouette Images. In *Int. Conf. on Machine Learning*.
- [12] Zhizhong Han, Chao Chen, Yu-Shen Liu, and Matthias Zwicker. 2020. ShapeCaptioner: Generative caption network for 3D shapes by learning a mapping from parts detected in multiple views to sentences. In *Proc. ACM Int. Conf. on Multimedia*. 1018–1027.
- [13] Zhizhong Han, Mingyang Shang, Xiyang Wang, Yu-Shen Liu, and Matthias Zwicker. 2019. Y2Seq2Seq: Cross-modal representation learning for 3D shape and text by joint reconstruction and prediction of view and word sequences. In *Proc. AAAI Conference on Artificial Intelligence*, Vol. 33. 126–133.
- [14] Zhizhong Han, Xiyang Wang, Yu-Shen Liu, and Matthias Zwicker. 2019. Multi-Angle Point Cloud-VAE: Unsupervised Feature Learning for 3D Point Clouds from Multiple Angles by Joint Self-Reconstruction and Half-to-Half Prediction. In *Proc. Int. Conf. on Computer Vision*.
- [15] Tao Hu, Zhizhong Han, Abhinav Shrivastava, and Matthias Zwicker. 2019. Render4Completion: Synthesizing Multi-view Depth Maps for 3D Shape Completion. *arXiv preprint arXiv:1904.08366* (2019).
- [16] Tao Hu, Zhizhong Han, and Matthias Zwicker. 2019. 3D Shape Completion with Multi-view Consistent Inference. *arXiv preprint arXiv:1911.12465* (2019).
- [17] Zhibin Hu, Yongsheng Luo, Jiong Lin, Yan Yan, and Jian Chen. 2019. Multi-Level Visual-Semantic Alignments with Relation-Wise Dual Attention Network for Image and Text Matching. In *Proc. Int. Joint Conf. on Artificial Intelligence*. 789–795.
- [18] Eldar Insafutdinov and Alexey Dosovitskiy. 2018. Unsupervised Learning of Shape and Pose with Differentiable Point Clouds. *Advances in Neural Information Processing Systems* (2018), 2807–2817.
- [19] Kalervo Järvelin and Jaana Kekäläinen. 2002. Cumulated gain-based evaluation of IR techniques. *ACM Trans. Information Systems* 20, 4 (2002), 422–446.
- [20] Z. Ji, H. Wang, J. Han, and Y. Pang. 2020. SMAN: Stacked Multimodal Attention Network for Cross-Modal Image-Text Retrieval. *IEEE Trans. Cybernetics* (2020), 1–12.
- [21] Andrej Karpathy and Li Fei-Fei. 2015. Deep visual-semantic alignments for generating image descriptions. In *Proc. IEEE Conf. on Computer Vision & Pattern Recognition*. 3128–3137.
- [22] Andrej Karpathy, Armand Joulin, and Li Fei-Fei. 2014. Deep fragment embeddings for bidirectional image sentence mapping. *Advances in Neural Information Processing Systems* 27 (2014), 1889–1897.
- [23] Diederik P. Kingma and Jimmy Ba. 2015. Adam: A Method for Stochastic Optimization. In *Proc. Int. Conf. on Learning Representations*.
- [24] Ryan Kiros, Ruslan Salakhutdinov, and Richard S Zemel. 2014. Unifying visual-semantic embeddings with multimodal neural language models. *arXiv preprint arXiv:1411.2539* (2014).
- [25] Kuang-Huei Lee, Xi Chen, Gang Hua, Houdong Hu, and Xiaodong He. 2018. Stacked cross attention for image-text matching. In *Proc. Euro. Conf. on Computer Vision*. 201–216.
- [26] Kuang-Huei Lee, Hamid Palangi, Xi Chen, Houdong Hu, and Jianfeng Gao. 2019. Learning visual relation priors for image-text matching and image captioning with neural scene graph generators. *arXiv preprint arXiv:1909.09953* (2019).
- [27] Yangyan Li, Rui Bu, Mingchao Sun, Wei Wu, Xinhan Di, and Baoquan Chen. 2018. Pointcnn: Convolution on x-transformed points. *Advances in Neural Information Processing Systems* 31 (2018), 820–830.
- [28] Xinhai Liu, Zhizhong Han, Yu-Shen Liu, and Matthias Zwicker. 2019. Point2Sequence: Learning the Shape Representation of 3D Point Clouds with an Attention-based Sequence to Sequence Network. In *Proc. AAAI Conference on Artificial Intelligence*. 8778–8785.
- [29] Xinhai Liu, Zhizhong Han, Wen Xin, Yu-Shen Liu, and Matthias Zwicker. 2019. L2G Auto-encoder: Understanding Point Clouds by Local-to-Global Reconstruction with Hierarchical Self-Attention. In *Proc. ACM Int. Conf. on Multimedia*.
- [30] Junhua Mao, Wei Xu, Yi Yang, Jiang Wang, and Alan L. Yuille. 2015. Deep Captioning with Multimodal Recurrent Neural Networks (m-RNN). In *Proc. Int. Conf. on Learning Representations*.
- [31] Kaichun Mo, Shilin Zhu, Angel X Chang, Li Yi, Subarna Tripathi, Leonidas J Guibas, and Hao Su. 2019. Partnet: A large-scale benchmark for fine-grained and hierarchical part-level 3d object understanding. In *Proc. IEEE Conf. on Computer Vision & Pattern Recognition*. 909–918.
- [32] Charles R Qi, Hao Su, Kaichun Mo, and Leonidas J Guibas. 2017. Pointnet: Deep learning on point sets for 3d classification and segmentation. In *Proc. IEEE Conf. on Computer Vision & Pattern Recognition*. 652–660.
- [33] Charles Ruizhongtai Qi, Li Yi, Hao Su, and Leonidas J Guibas. 2017. Pointnet++: Deep hierarchical feature learning on point sets in a metric space. *Advances in Neural Information Processing Systems* 30 (2017), 5099–5108.
- [34] Florian Schroff, Dmitry Kalenichenko, and James Philbin. 2015. FaceNet: A unified embedding for face recognition and clustering. In *Proc. IEEE Conf. on Computer Vision & Pattern Recognition*. 815–823.
- [35] Bokun Wang, Yang Yang, Xing Xu, Alan Hanjalic, and Heng Tao Shen. 2017. Adversarial Cross-Modal Retrieval. In *Proc. ACM Int. Conf. on Multimedia*. 154–162.
- [36] Yaxiong Wang, Hao Yang, Xueming Qian, Lin Ma, Jing Lu, Biao Li, and Xin Fan. 2019. Position Focused Attention Network for Image-Text Matching. In *Proc. Int. Joint Conf. on Artificial Intelligence*. 3792–3798.
- [37] Xin Wen, Zhizhong Han, Geunhyuk Youk, and Yu-Shen Liu. 2020. CF-SIS: Semantic-Instance Segmentation of 3D Point Clouds by Context Fusion with Self-Attention. In *Proc. ACM Int. Conf. on Multimedia*.
- [38] Xin Wen, Tianyang Li, Zhizhong Han, and Yu-Shen Liu. 2020. Point Cloud Completion by Skip-attention Network with Hierarchical Folding. In *Proc. IEEE Conf. on Computer Vision & Pattern Recognition*.
- [39] Wenxuan Wu, Zhongang Qi, and Li Fuxin. 2019. Pointconv: Deep convolutional networks on 3d point clouds. In *Proc. IEEE Conf. on Computer Vision & Pattern Recognition*. 9621–9630.
- [40] Xing Xu, Tan Wang, Yang Yang, Lin Zuo, Fumin Shen, and Heng Tao Shen. 2020. Cross-Modal Attention With Semantic Consistence for Image-Text Matching. *IEEE Trans. Neural Networks and Learning Systems* 31, 12 (2020), 5412–5425.
- [41] Matthew D Zeiler. 2012. Adadelta: an adaptive learning rate method. *arXiv preprint arXiv:1212.5701* (2012).
- [42] Ying Zhang and Huchuan Lu. 2018. Deep Cross-Modal Projection Learning for Image-Text Matching. In *Proc. Euro. Conf. on Computer Vision*, Vol. 11205. 707–723.